İSTANBUL
UNIVERSITY
P R E S S

DIRECTED EVOLUTION OF AN ONCOLYTIC VESICULAR STOMATITIS VIRUS ADAPTED TO HUMAN MALIGNANT MENINGIOMA CELLS

İNSAN MALIGANT MENİNJİOM HÜCRELERİNE UYUMLANMIŞ BİR ONKOLİTİK VEZİKÜLER STOMATİT VİRÜSÜNÜN YÖNLENDİRİLMİŞ EVRİMİ

Burak Gizem GÖLEŞ[1,2] , **Hülya YAZICI**[3] , **John N. DAVIS**[4]

[1]İstanbul University, Institute of Oncology, Department of Basic Oncology, Division of Cancer Genetics, İstanbul, Türkiye
[2]İstanbul University, Institute of Graduate Studies in Health Sciences, Department of Basic Oncology, İstanbul, Türkiye
[3]İstanbul Arel University, Faculty of Medicine, Department of Medical Biology and Genetics, İstanbul, Türkiye
[4]Yale University School of Medicine, Department of Neurosurgery, New Haven, CT, USA

ORCID ID: B.G.G. 0000-0001-7990-4878; H.Y. 0000-0002-8919-0482; J.N.D. 0000-0003-2851-644X

ABSTRACT

Objectives: Recombinantly-engineered versions of the oncolytic virus VSV are currently under clinical investigation for the treatment of several different types of cancer. Here we aim to enhance the cancer-killing oncolytic phenotype of VSV-1'GFP toward human malignant meningioma cells using a directed evolution approach.

Material and Methods: Two independent trials of repeated growth of VSV-1'GFP on cultures of meningioma IOMM-Lee cells were performed. This adaptation procedure allows for the selection of viral mutants that display an enhanced oncolytic phenotype. A fluorescent viral plaque assay was used to measure changes in plaque size indicative of enhanced viral growth on these cancer cells. Sanger sequencing was used to identify the viral mutations responsible.

Results: Adapted VSV-1'GFP from each of the growth trials yielded larger fluorescent plaques than control virus, indicating the emergence of viral mutants with increased growth on these meningioma cells. Plaques from adapted virus were 184%±9% (Trial 1) and 166%±7% (Trial 2) larger than control (n=60; p<0.001; ANOVA). Sequencing determined that adapted virus from Trial 1 harbored 3 mutations: a silent mutation Y178Y in the M gene, an E92K mutation in the G gene, and a K152R mutation in the L gene. Trial 2 yielded 3 mutations in the G gene: N36T, E92K, and E254K.

Conclusion: The E92K mutation of the viral G-protein emerged independently in both growth trials, suggesting that this change may play a role in producing the enlarged-plaque phenotype and enhanced oncolytic propagation in IOMM-Lee cells. Further investigations of the prospect for treating malignant meningiomas using VSV-based oncolytic virotherapy appear warranted and, to the best of our knowledge, the present study appears to be the first directed evolution experiment involving an oncolytic virus adapted to human meningioma cells.

Keywords: Vesicular stomatitis virus, oncolytic virus, meningioma, mutagenesis

ÖZ

Amaç: Onkolitik virüs VSV'nin rekombinant olarak tasarlanmış çeşitleri birkaç farklı kanser türünün tedavisi için klinik olarak araştırılmaktadır. Bu çalışmada, yönlendirilmiş evrim yaklaşımı kullanarak VSV-1'GFP' nin insan malign meninjiyom hücrelerine yönelik kanser öldürücü onkolitik fenotipini geliştirmek hedeflenmektedir.

Gereç ve Yöntemler: Meninjiyom IOMM-Lee hücrelerinin kültürleri üzerinde VSV-1'GFP'nin tekrarlanan büyümesine ilişkin iki bağımsız deneme gerçekleştirildi. Bu adaptasyon prosedürü, gelişmiş bir onkolitik fenotip gösteren viral mutantların seçimine olanak tanır. Bu kanser hücrelerinde viral büyümenin arttığını gösteren plak boyutundaki değişiklikleri ölçmek için bir floresan viral plak tahlili kullanıldı. Sorumlu viral mutasyonları tanımlamak için Sanger dizilimi kullanıldı.

Bulgular: Büyüme denemelerinin her birinden uyarlanmış VSV-1'GFP, kontrol virüsünden daha büyük floresan plaklar verdi; bu, meninjiyom hücrelerinde artan büyüme ile viral mutantların ortaya çıktığını gösterir. Uyarlanmış virüsten alınan plaklar kontrolden (n=60; p<0,001; ANOVA) %184±%9 (Deneme 1) ve %166±%7 (Deneme 2) daha büyüktü. Dizileme, Deneme 1'den uyarlanan virüsün 3 mutasyon barındırdığını belirledi: M geninde sessiz bir Y178Y mutasyonu, G geninde bir E92K mutasyonu ve L geninde bir K152R mutasyonu. Deneme 2, G geninde 3 mutasyon ortaya çıkardı: N36T, E92K ve E254K.

Sonuç: Viral G-proteininin E92K mutasyonu, her iki büyüme denemesinde de bağımsız olarak ortaya çıktı; bu değişiklik, IOMM-Lee hücrelerinde genişlemiş plak fenotipinin ve gelişmiş onkolitik yayılımın üretilmesinde rol oynayabileceğini düşündürmektedir. Malign meninjiyomların VSV bazlı onkolitik viroterapi kullanılarak tedavi edilmesi olasılığına ilişkin daha fazla araştırma gerekli görülmektedir ve bilgimiz dâhilinde, mevcut çalışma, insan meninjiyom hücrelerine uyarlanmış bir onkolitik virüsü içeren ilk yönlendirilmiş evrim deneyi olarak literatüre katkı sunmaktadır.

Anahtar Kelimeler: Veziküler stomatit virüs, onkolitik virüs, meninjiom, mutagenez

INTRODUCTION

Oncolytic viruses are a heterogenous collection of recombinant viruses that have been engineered to selectively target, infect, and ultimately kill cancer cells; hence the term oncolytic (onco=cancer; lytic=lysis) that is commonly used to describe them (1, 2). Several different oncolytic viruses are currently under investigation for clinical application in the treatment of cancer (1, 2). In these experimental oncolytic virotherapy treatment regimens, the virus is typically injected directly into the solid tumor mass, where it initially infects a small fraction of tumor cells. Over the course of several hours, the virus replicates and new daughter viruses are released from these infected cells to continue further cycles of viral infection and replication throughout the tumor mass. Since the virus seizes control of all the intracellular translation machinery to make more copies of itself, infected cancer cells ultimately die (oncolysis). Recombinantly-engineered poliovirus, measles, and herpes simplex viruses have all been the focus of clinical trials aimed at examining the safety and efficacy of these agents in targeting and eliminating glioblastoma, multiple myeloma, and melanoma, in addition to several other types of cancer (3-5). In 2015, the Food and Drug Administration (FDA) of the United States approved the first oncolytic virus, talimogene laherparepvec (T-Vec), for use in the treatment of inoperable late-stage melanoma (6). Another oncolytic virus with therapeutic prospects that has been the focus of much interest is vesicular stomatitis virus (VSV) (7, 8). VSV is an enveloped, non-segmented ssRNA(-) virus from the family *Rhabdoviridae* with human infections generally presenting as either asymptomatic or with mild flu-like symptoms (Figure 1) (9). To date, a wide assortment of recombinant VSVs have been generated and tested for their oncolytic properties *in vitro*, with several showing therapeutic potential *in vivo* using both immune-compromised animals implanted with human tumors and immune-competent (syngeneic) animal tumor models (10-14). Efforts have also been made to exploit the highly-mutagenic nature of this class of ssRNA(-) virus by adapting recombinant oncolytic VSVs for growth on cultures of specific types of cancer cells, e.g. pancreatic cancer, breast cancer, and glioblastoma cells (15-18). These directed evolution strategies of viral mutagenesis aim to select mutant cancer-specific variants of VSV that exhibit an enhanced oncolytic phenotype targeting the cancer of interest.

Here we describe a directed evolution experiment utilizing the recombinant oncolytic virus VSV-1'GFP to target cultures of the immortalized human malignant meningioma cell line IOMM-Lee. Meningiomas are the most frequently encountered type of primary brain tumor and although the majority of these tumors are benign, a small subset is highly-aggressive and result in significant morbidity (19, 20). Several genes have been identified as playing a role in meningioma oncogenesis and include *NF2, TRAF7, KLF4, AKT1*, among others (21, 22). The IOMM-Lee cell line utilized in the present study was initially established from a freshly-resected intraosseous malignant meningioma of the skull taken from a 61-year old male (23, 24). Multiple passages of VSV-1'GFP on cultures of these cells resulted in the emergence of an enhanced oncolytic phenotype accompanied by several mutations of the viral genome that were identified through Sanger sequencing.

MATERIALS and METHODS

Cell cultures and recombinant virus

The human malignant meningioma IOMM-Lee cell line utilized in the present study was a kind gift from the laboratory of M. Gunel (Yale University School of Medicine). Cells were cultured using Dulbecco's Modified Eagle Medium cat no. 11965-092 (Gibco/ThermoFisher Scientific, Waltham, MA, USA) supplemented with 10% FBS cat no. 16000-044 (Gibco) and 1% Pen-Strep solution cat no. 15140-122 (Gibco) (23-25). Cultures were maintained in an incubator with a humidified atmosphere at 37°C supplemented with 5% CO_2.

The recombinant oncolytic virus VSV-1'GFP was a kind gift from the laboratory of S. Whelan (Washington University School of Medicine in St. Louis). This virus was engineered to expresses green fluorescent protein (GFP) from the first (1') genomic position. Virus was grown and harvested as described previously (26, 27).

Repeated passage experiments

The day before infection, IOMM-Lee cells were seeded into 35 mm dishes or wells at a density of 5.0×10^5. The following day, nearly confluent cultures were inoculated with virus and incubated 1 hr to allow time for viral adsorption and infection. After incubation, the inoculum was removed, the cells were washed with PBS, and fresh medium was added before returning the cultures to the incubator. After 24 hrs, cultures were observed under fluorescent microscopy and a sample of media containing newly generated viral progeny was drawn and used as inoculum to infect a fresh set of cultures. Remaining medium was harvested and stored at -80°C for later analysis. This repeated passage procedure was continued for 22-24 cycles of infection.
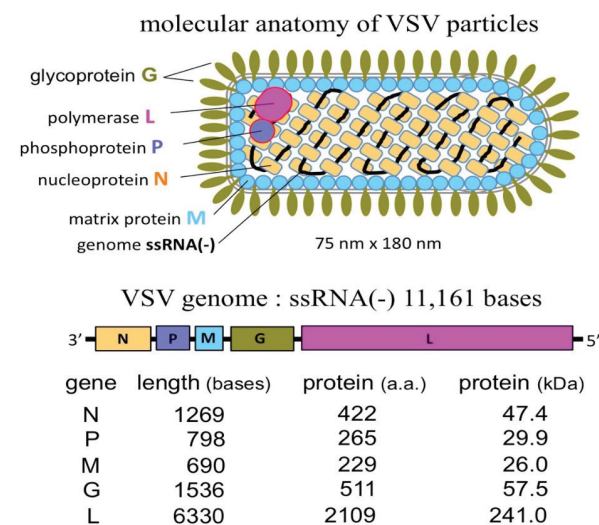

Figure 1: Molecular characteristics of vesicular stomatitis virus (VSV). Illustration showing molecular anatomy of VSV particles (top) and organization of VSV genome (below)

molecular anatomy of VSV particles

glycoprotein **G**
polymerase **L**
phosphoprotein **P**
nucleoprotein **N**
matrix protein **M**
genome **ssRNA(-)**

75 nm x 180 nm

VSV genome : ssRNA(-) 11,161 bases

3' N P M G L 5'

gene	length (bases)	protein (a.a.)	protein (kDa)
N	1269	422	47.4
P	798	265	29.9
M	690	229	26.0
G	1536	511	57.5
L	6330	2109	241.0

The initial VSV-1'GFP inoculum used to infect the first culture (p0) consisted of a 15 µL volume containing 2.4×10^6 infectious virions. In subsequent passages, the volume of viral inoculum was varied in response to the observed viral propagation of the previous passage.

Plaque-size assay and fluorescent imaging

VSV-1'GFP expresses GFP as a reporter protein, thus, fluorescent imaging was used to determine the size of viral plaques that develop on infected cell monolayers in a plaque assay (12, 28). Briefly, confluent monolayers of IOMM-Lee cells grown in 6-well plates were inoculated using 1 mL volumes of serially-diluted virus and allowed to incubate at 37 °C for one hour. After adsorption, the viral inoculum in each well was aspirated and cell monolayers were overlaid with 2 ml of 0.5% (wt/vol) Ultrapure GPG/LE agarose cat no. AB00972 (American Bioanalytical, Natick, MA, USA) that had been melted and mixed with growth medium. After 3-5 min of solidification, the overlaid plates were returned to the 37 °C incubator for 24 hrs to allow time for viral plaque development.

Visualization of fluorescent plaques and infected cell monolayers was performed using an inverted IX71 fluorescent microscope system (Olympus, Tokyo, Japan) fitted with a GFP filter set. Images were captured using a SPOT digital camera (Diagnostic Instruments, Sterling Heights, MI, USA) and further processed using Adobe Photoshop 7.0 (Adobe Systems, San Jose, CA, USA). Individual fluorescent plaques were measured across their diameter directly from a computer monitor and 60 plaques were randomly measured from each experimental condition to determine the mean plaque-size of the population.

Viral genome sequencing

Viral genomic RNA for sequencing was isolated from the culture medium of infected cells using the QIAamp Viral RNA Mini Kit cat no. 52904 (QIAGEN, Germantown, MD, USA). This RNA was then used as template for generating cDNAs in a reverse-transcription reaction with SMARTScribe Reverse Transcriptase cat no. 639537 (Takara Bio, San Jose, CA, USA). The oligos AF00001 and DF04742 were used in these reactions (RT1, RT2). Viral genomic cDNAs were then used to generate a series of seven overlapping PCR products (A, B, C, D, E, F, and G), covering the length of the VSV-1'GFP genome. These PCR products ranged in size from 1.5 – 2.3 kb and were generated using the Phusion High-Fidelity PCR Master Mix kit cat no. M0531S (New England Biolabs, Ipswich, MA, USA). The annealing temperatures used for Phusion High-Fidelity PCR were calculated using the online NEB Tm Calculator at the New England Biolabs website (tmcalculator.neb.com). After amplification, PCR products were purified using the QIAquick PCR Purification kit cat no. 28104 (QIAGEN), mixed with sequencing primer, then submitted to the Keck DNA Sequencing Facility (Yale University School of Medicine, New Haven, CT, USA) for automated DNA sequencing. All oligos were synthesized by IDT (Integrated DNA Technologies, Inc., Research Triangle Park, NC, USA) . The numbering associated with each oligo is indicative of the nucleotide position in the original recombinant VSV genome (29). Recombinant VSV

reference sequence used in the design of oligos and primers was obtained from plasmid # 31833 available on the Addgene website (www.addgene.org). VSV glycoprotein sequence of the wild-type Orsay strain of Indiana serotype VSV was obtained from GenBank Accession: M11048 (30). Initial sequencing of the G gene of the founder stock of VSV-1'GFP immediately after arrival in the lab found that there are five variations in the founder sequence relative to the GenBank M11048 sequence, i.e. c.3918A>G, (p.Gln26Arg); c.4115A>G, (p.Lys92Glu); c.4440C>T, (p.Thr200Met); c.5022T>C, (p.Leu394Ser) and c.5247T>G, (p.Phe469Cys). At this time, it is unclear whether these variations were present in the original VSV-1'GFP plasmid construct used to generate the virus or emerged later during standard harvesting and maintenance of viral stocks.

Statistical analysis

Fluorescent plaque-size data were compared using a one-way Analysis of Variance statistical model (ANOVA), followed by post-hoc analysis (Bonferroni's test) and were computed using the InStat version 3.0b software package (GraphPad Software, Boston, MA, USA). P-values <0.05 were considered significant.

RESULTS

Repeated passage of virus using IOMM-Lee cells

Cultures of human malignant meningioma IOMM-Lee cells were inoculated with VSV-1'GFP and incubated for 24 hrs to allow time for viral propagation (Figure 2). Since VSV-1'GFP expresses green fluorescent protein (GFP) as a reporter molecule, the extent of viral infection in IOMM-Lee cultures was easily monitored using fluorescent microscopy. After 24 hrs, a sample of inoculum containing newly generated viral progeny was collected and used to infect fresh IOMM-Lee cultures (Figure 2). Two independent trials (performed serially) of this repeated passage procedure were conducted with Trial 1 consisting of 24 passages and Trial 2 consisting of 22. During the
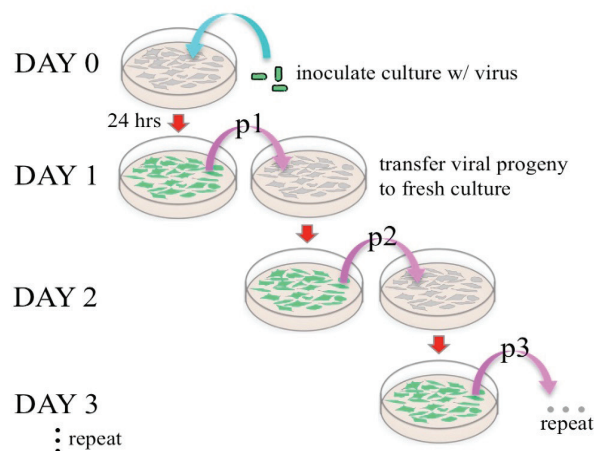

Figure 2: Directed evolution of VSV-1'GFP by repeated passage. Diagram depicting inoculation of IOMM-Lee cells with virus and transfer of newly generated viral progeny to fresh cultures after 24 hrs

course of these trials, robustly infected cultures prompted the use of smaller volumes of inoculum (one-half to one-third) in the next subsequent passage (Figure 3, left). Likewise, weakly infected cultures prompted the use of greater volumes of inoculum (Figure 3, center). The rationale behind this strategy was aimed at maximizing the potential number of cycles of viral replication per passage. A culture that becomes fully infected within the first few hours after inoculation leaves few remaining host cells available for infection and further cycles of viral replication. Thus, an oversupply of infectious virions at the outset of a passage might be expected to slow the emergence of new mutations and their fixation within the viral population.

cDNAs. The first cDNA (RT 1) included the GFP reporter gene and the viral N, P, M, and G genes. The second cDNA (RT 2) contained the viral polymerase L gene. RT 1 cDNA was then used as template to generate 3 overlapping PCR products (A, B, C) spanning the length of RT 1; RT 2 was used as template for 4 PCR products (D, E, F, G). Sanger sequencing was then used to sequence all PCR products. After assembly and inspection of the sequencing chromatograms, several mutations were identified in the genomes of the late-passage virus from both trials (Figure 6). Late-passage virus (p24) in Trial 1 harbored 3 mutations: a silent mutation Y178Y in the M gene and two amino acid altering mutations, E92K in the G gene and K152R
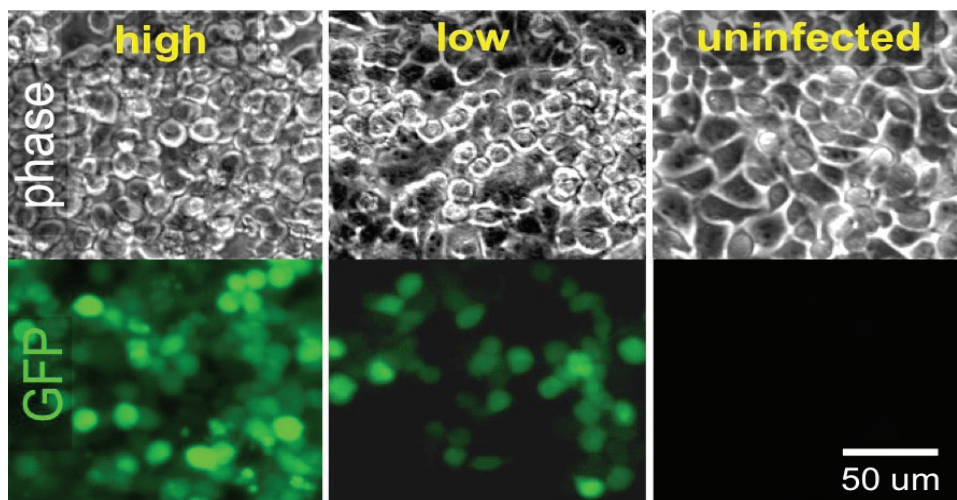

Figure 3: Infection of IOMM-Lee cells with VSV-1'GFP. Phase-contrast (above) and fluorescent images (below) of infected cultures. Highly infected culture (left) displays numerous rounded cells due to cellular cytopathic effects (CPE) of infection. Less infected culture (center) displays fewer CPE and fewer GFP positive cells. Uninfected culture (right) included as control

Altered phenotype: Viral plaque-size
The application of a semi-solid agarose overlay restricts the diffusion of newly generated viral progeny to an area immediately surrounding the initial infected host cell and, over the course of hours, results in the development of a viral plaque or circular-shaped area of robustly infected cells (28). Using confluent cultures of IOMM-Lee cells, we compared the size of fluorescent viral plaques that developed after infection with early- (p1) and late- (p24 and p22) passage viral inoculum harvested from both repeated passage trials (Figure 4). In both Trial 1 and Trial 2, late-passage virus yielded larger fluorescent plaques than early-passage virus; late-passage plaques were 184% ± 9% and 166% ± 7% larger, respectively (n=60; p<0.001; ANOVA).

Altered genotype: VSV-1'GFP mutations
Next we decided to perform whole viral genome sequencing to determine what mutations had emerged in VSV-1'GFP that might account for the enlarged fluorescent plaque phenotype (Figure 5). Viral genomic RNA was extracted from both early- (p1) and late- (p24 and p22) passage virus from both trials and reverse-transcribed into two overlapping single-stranded

in the L gene. Trial 2 late-passage virus (p22) also harbored 3 mutations that all altered amino acids within the G gene: N36T, E92K, and E254K. Sequences of the early-passage (p1) virus from both trials matched each other and pre-existing sequence of the original founder stocks. Interestingly, some regions of the late-passage genomic sequence from both trials appeared to harbor what may be additional mutations that have not yet become genetically fixed in the viral population (e.g. Figure 6 p22 in K152R column). However, it is unclear from the sequencing chromatograms alone what fraction of the virions in the population may possess these types of alterations.

DISCUSSION

A common feature among RNA viruses is their ability to mutate very quickly (31). This high frequency of mutagenesis is understood to arise from a lack of proof-reading activity by the virally-encoded RNA polymerases responsible for replicating the viral genome (32, 33). For VSV, this RNA polymerase is encoded by the L gene and has been estimated to yield mutation rates as high as one mutation per genome per replication cycle (34, 35). Additionally, measurements of recombinant VSV growth kinetics *in vitro* indicate that the time between initial cellular
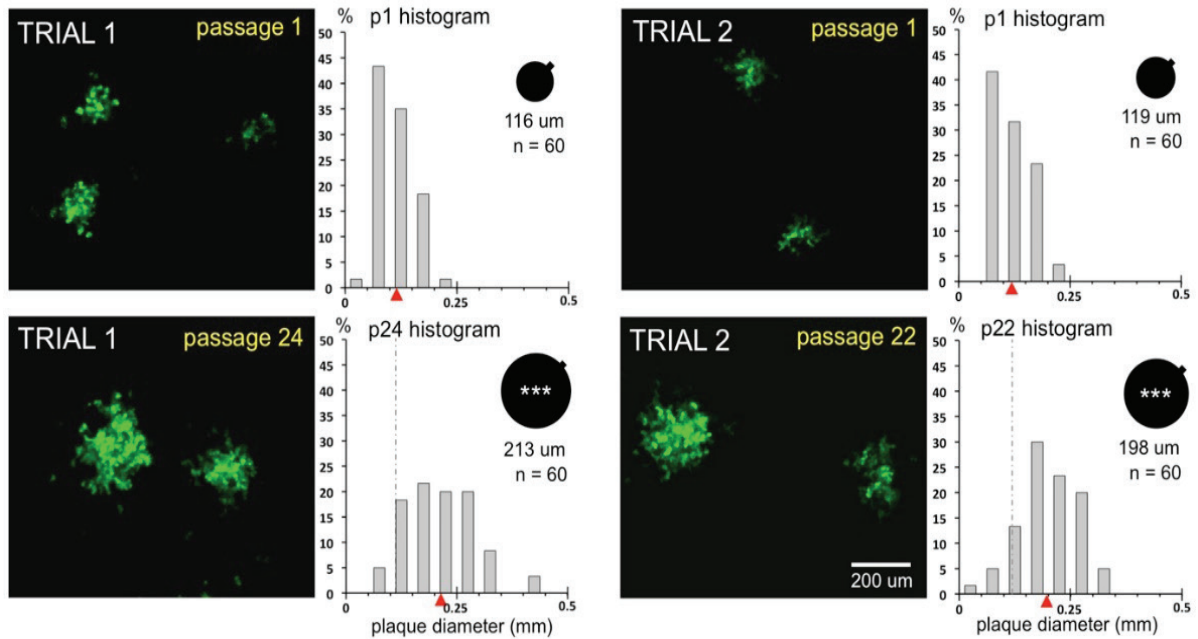
Figure 4: Viral plaque-size assay of early- and late-passage VSV-1'GFP. Fluorescent plaques were imaged 24 hrs after infection and agarose overlay of IOMM-Lee cells. Trials 1 and 2 are shown (left and right, respectively). Plaques from later passages (p24, p22; bottom) are larger than initial passage (p1; top). Size measurements (n=60 plaques per condition) indicate a significant increase (p<0.001; ANOVA) in plaque size. Circles depict mean plaque-size with standard error (small projection) and histograms depict plaque-size distribution (red markers indicate mean)
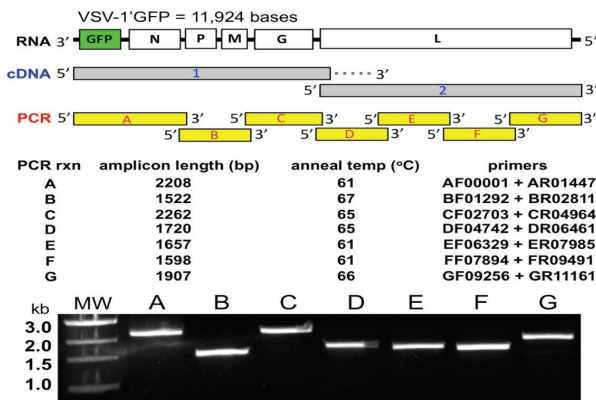

Figure 5: PCR-based VSV-1'GFP sequencing strategy. Illustration (top) shows VSV RNA genome, cDNA products (#1 and #2 generated by reverse-transcription with oligos AF00001 and DF04742, respectively), and resulting PCR products (A, B, C, D, E, F, G) generated using high-fidelty PCR. PCR reactions and conditions are listed (center). Agarose gel of purified PCR products (bottom)

infection and release of new viral progeny (the latency period) ranges from 2-3 hrs (12, 36). Thus, over the course of a 24 hr period, one might expect 8 to 12 cycles of VSV replication to occur. Finally, single cell analysis suggests that, after infection and prior to cell death, nearly 1,000-2,000 new progeny VSV virions can be released from a single infected host cell (37). The high VSV mutation rate, fast replication kinetics, and robust release of progeny virions all contribute to the production of a genetically diverse VSV population that is highly adaptable

and amenable to experiments involving artificial selection, as demonstrated by the directed evolution experiment of the present study.

Of the four amino acid altering mutations that emerged in VSV-1'GFP after repeated passage on IOMM-Lee cultures, three (N36T, E92K, and E254K) were localized to the G gene, with the E92K mutation emerging twice, independently in both trials. While cross-contamination between cultures and experiments is always a concern, this explanation for the presence of E92K in both trials can be excluded due to the presence of the silent Y178Y mutation found in the M gene from Trial 1, yet absent from the sequence of Trial 2. Despite being conducted serially rather than in parallel, if cross-contamination between the trials had somehow occurred, then this silent mutation from the first trial would also have been carried over into the second trial. Thus, the E92K mutation appears to have emerged independently in both trials and may be playing a role in producing the enlarged-plaque phenotype observed in the plaque-size assay.

The VSV glycoprotein or G-protein encoded by the G gene is an integral membrane protein localized to the plasma membrane enveloping the VSV virion. This protein is responsible for the initial attachment and fusion of the virus with the host cell and is critical to host cell entry, infection, and continued propagation (9, 38). Since the G-protein plays such an integral role in the VSV replication cycle, even minor changes to the amino acid sequence might be expected to measurably influence the growth and size of viral plaques in the context of a plaque-size assay. Interestingly, the wild-type sequence of the Orsay strain of Indiana serotype
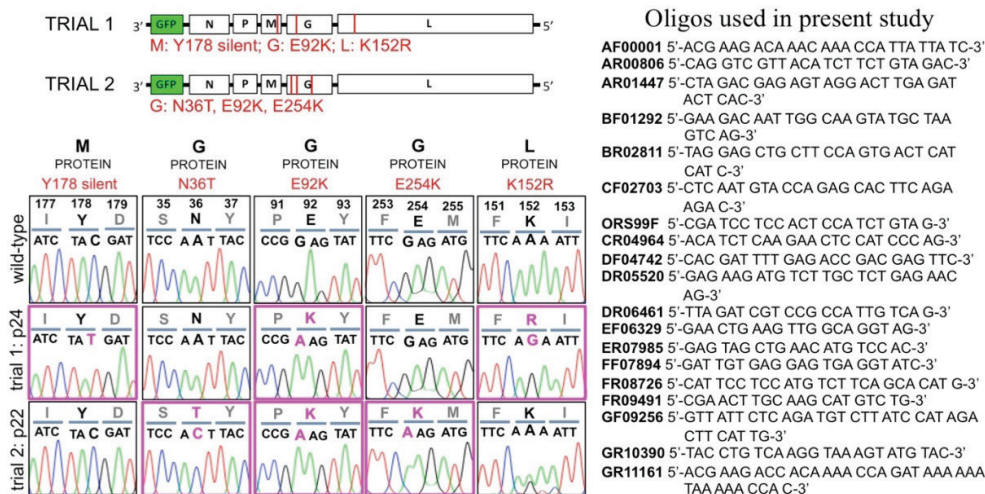
Figure 6: Mutations identified in late-passage VSV-1'GFP genomes. Diagram showing genomic location of mutations that emerged after repeated passage in each trial (top left). Sequence chromatograms (bottom left) from wild-type and late-passage virus covering each mutation site. Nucleotides and amino acids differing from wild-type are highlighted in magenta. Sequences of oligos used for RT, PCR, and automated DNA sequencing are also listed (right)

VSV (GenBank Accession: M11048) from which the VSV-1'GFP G-protein is derived, codes for a lysine (K) at codon 92, the same as that found in both of our IOMM-Lee derived late-passage mutants. Initial sequencing of the G-protein in the founder stock of VSV-1'GFP immediately after arrival in the laboratory indicated several deviations from the M11048 sequence (see Methods), one of which was the substitution of glutamate (E) at codon 92. At this time, it is unclear whether these variations were present in the original VSV-1'GFP plasmid construct used to first generate the virus, or emerged some time later during standard maintenance of viral stocks. To replenish viral stocks, VSV is most frequently grown and harvested from infected cultures of BHK-21 cells (baby hamster kidney cells) or Vero cells (African green monkey kidney cells). Both of these cell lines harbor defects of their innate immune system, making them highly permissive cellular hosts suitable for the maintenance propagation of viruses (39, 40). One possibility is that VSV-1'GFP was originally generated using the wild-type K92 codon and, through repeated maintenance propagation on either BHK-21 or Vero cells lacking a functional innate immune system, mutated to become the E92 variant found in our VSV-1'GFP founder stocks. Repeated passage on IOMM-Lee cells, which appear to display at least a partially functional innate immune response, may have simply re-introduced a wild-type selection pressure that shifted the viral population back to the original wild-type codon of K92 (41). Further work will be necessary to determine what role, if any, innate immune effects might play in the emergence, or loss, of the E92K mutation.

Recently, a directed evolution experiment involving two different oncolytic VSVs (VSV-p53wt and VSV-p53-CC) was reported in which 33 repeated passages were used to adapt each virus to pancreatic cancer cells (18). Interestingly, after sequencing each of the adapted viral genomes, a pair of G-protein mutations (K174E and E238K) were found to have emerged in both of these independently adapted viruses. Whereas, in the context of this single study, one might argue that a pair of mutations involving the same two amino acids, i.e. glutamate (E) and lysine (K), may simply be a coincidence, this same reasoning becomes less plausible when we also consider the E92K and E254K mutations found in our IOMM-Lee adapted VSV-1'GFP. The Orsay VSV G-protein is assembled from 511 amino acids, of which 26 (5.1%) are glutamate (E) and 30 (5.9%) are lysine (K). Given a single E or K residue taken from a pool of the 511 Orsay G-protein residues, the probability of randomly drawing a second E or K is 55/510 or 10.8%. The probability of randomly drawing a pair of E or K residues from two duplicate pools in only two draws from each pool is $[(56/511)(55/510)]^2$ or 0.0014%. At neutral pH, both glutamate and lysine are charged molecules with glutamate being negative (-E) and lysine positive (+K). It has been suggested that the K174E and E238K mutations might improve virus entry into pancreatic cancer cells due to their proximity to the region of the G-protein that undergoes a large conformational rearrangement during the process of virion fusion with the endosomal membrane (17). A similar argument could potentially be made for the E92K and E254K mutations and IOMM-Lee cells. Since this fusion event is triggered by acidification of the endosome, mutations in this region of the G-protein that result in a substitution with an oppositely charged amino acid (e.g. -E ⇒ +K) may influence the sensitivity of this triggering mechanism (42, 43). Taken together, the finding that cells from two very different types of cancer, i.e. pancreatic cancer and malignant meningioma, both yielded pairs of E/K mutations localized to the same region of a single protein warrants further investigation. Additional work examining the influence of extracellular pH on these, and similar G-protein mutants may prove informative.

Finally, the N36T mutation of the G-protein in Trial 2 and the K152R mutation of the L-protein in Trial 1 appear to have no

obvious basis for comparison in the literature. However, the sequencing chromatogram for the K152R site from Trial 2 is suggestive of a heterogenous population of virions, some with the K152R mutation and some without (Figure 6 p22 in K152R column). This apparently mixed population of mutant and wild-type virions may indicate the initial emergence of the K152R mutation in Trial 2, prior to becoming genetically fixed in the viral population, as it has in Trial 1. Newly-engineered recombinant VSVs (reverse-genetics) will be required to investigate which of the 4 amino acid altering mutations of the present study are necessary and sufficient for the production of the enlarged-plaque phenotype.

CONCLUSION

The present study demonstrates that *in vitro* directed evolution techniques can be applied to adapt mutation-prone oncolytic viruses for improved growth on cultures of human meningioma cells. After adaptation on IOMM-Lee cells in two independent trials, VSV-1'GFP was found harboring 3 non-synonymous mutations (N36T, E92K, E254K) of the glycoprotein (G) responsible for viral entry and 1 non-synonymous mutation (K152R) of the RNA polymerase protein (L) responsible for RNA synthesis and replication of the viral genome. One of these mutations (E92K) was found to have emerged independently in both adaptation trials, thus suggesting a role for this mutation in the production of the enlarged plaque-size phenotype found on IOMM-Lee cells. Further investigations of the prospect for treating malignant meningiomas using VSV-based oncolytic virotherapy appear warranted.

REFERENCES

1. Goradel NH, Baker AT, Arashkia A, Ebrahimi N, Ghorghanlu S, Negahdari B. Oncolytic virotherapy: Challenges and solutions. Curr Probl Cancer 2021;45(1):100639.

2. Wollmann G, Ozduman K, van den Pol AN. Oncolytic virus therapy for glioblastoma multiforme: concepts and candidates. Cancer J 2012;18:69-81.

3. Desjardins A, Gromeier M, Herndon JE, Beaubier N, Bolognesi DP, et al. Recurrent glioblastoma treated with recombinant poliovirus. N Engl J Med 2018;379(2):150-61.

4. Dispenzieri A, Tong C, LaPlant B, Lacy MQ, Laumann K, Dingli D, et al. Phase I trial of systemic administration of Edmonston strain of measles virus genetically engineered to express the sodium iodide symporter in patients with recurrent or refractory multiple myeloma. Leukemia 2017;31(12):2791-8.

5. Andtbacka RHI, Collichio F, Harrington KJ, Middleton MR, Downey G, et al. Final analyses of OPTiM: a randomized phase III trial of talimogene laherparepvec versus granulocyte-macrophage colony-stimulating factor in unresectable stage III-IV melanoma. J Immunother Cancer 2019;7(1):145.

6. Zhang T, Hong-Ting Jou T, Hsin J, Wang Z, Huang K, Ye J, et al. Talimogene Laherparepvec (T-VEC): A Review of the Recent Advances in Cancer Therapy. J Clin Med 2023;12(3):1098.

7. Zhang Y, Nagal BM. Immunovirotherapy based on recombinant vesicular stomatitis virus: Where are we? Front Immunol 2022;13:898631.

8. Bishnoi S, Tiwari R, Gupta S, Byrareddy SN, Nayak D. Oncotargeting by vesicular stomatitis virus (VSV): Advances in cancer therapy. Viruses 2018;10(2):90.

9. Rose JK, Whitt MA. Rhabdoviridae: The viruses and their replication. In: Knipe DM & Howley PM, editors. Fields Virology 4th Edition. Philadelphia: Lippincott Williams & Wilkins; 2001. p.1221-44.

10. Ozduman K, Wollmann G, Piepmeier JM, van den Pol AN. Systemic vesicular stomatitis virus selectively destroys multifocal glioma and metastatic carcinoma in brain. J Neurosci 2008;28(8):1882-93.

11. Wollmann G, Rogulin V, Simon I, Rose JK, van den Pol AN. Some attenuated variants of vesicular stomatitis virus show enhanced oncolytic activity against human glioblastoma cells relative to normal brain cells. J Virol 2010;84(3):1563-73.

12. van den Pol AN, Davis JN. Highly-attenuated recombinant vesicular stomatitis virus VSV-12'GFP displays immunogenic and oncolytic activity. J Virol 2013;87(2):1019-34.

13. Wollmann G, Davis JN, Bosenberg MW, van den Pol AN. Vesicular stomatitis virus variants selectively infect and kill human melanomas but not normal melanocytes. J Virol 2013; 87(12):6644-59.

14. van den Pol AN, Zhang X, Lima E, Pitruzzello M, Albayrak N, et al. Lassa-VSV chimeric virus targets and destroys human and mouse ovarian cancer by direct oncolytic action and by initiating an anti-tumor response. Virology 2021;555:45-55.

15. Wollmann G, Tattersall P, van den Pol AN. Targeting human glioblastoma cells: Comparison of nine viruses with oncolytic potential. J Virol 2005;79(10):6005-22.

16. Gao Y, Whitaker-Dowling P, Watkins SC, Griffin JA, Bergman I. Rapid adaptation of a recombinant vesicular stomatitis virus to a targeted cell line. J Virol 2006;80(17):8603-12.

17. Garijo R, Hernandez-Alonso P, Rivas C, Diallo J-S, Sanjuan R. Experimental evolution of an oncolytic vesicular stomatitis virus with increased selectivity for p53-deficient cells. PloS One 2014;9(7):e102365.

18. Seegers SL, Frasier C, Greene S, Nesmelova IV, Grdzelishvili VZ.

Experimental evolution generates novel oncolytic vesicular stomatitis viruses with improved replication in virus-resistant pancreatic cancer cells. J Virol 2020;94(3):e01643-19.

19. Ozduman K, Wollmann G, Piepmeier JM. Gene therapy for meningiomas. In: Pamir MN, Black PM, Fahlbusch R, editors. Meningiomas: A comprehensive text. Philadelphia: Saunders-Elsevier; 2010. p.681-90.

20. Moliterno J, Omuro A, editors. Meningiomas: Comprehensive strategies for management. Springer-Nature Switzerland AG;2020. p.35-41.

21. Clark VE, Erson-Omay EZ, Serin A, Yin J, Cotney J, Ozduman K, et al. Genomic analysis of non-NF2 meningiomas reveals mutations in TRAF7, KLF4, AKT1, and SMO. Science 2013399(6123):1077-80.

22. Youngblood MW, Gunel M. Molecular genetics of meningiomas. Handb Clin Neurol 2020;169:101-9.

23. Lee WH, Tu YC, Liu MY. Primary intraosseus malignant meningioma of the skull: Case report. Neurosurgery 1988;23(4):505-8.

24. Lee WH. Characterization of a newly established malignant meningioma cell line of the human brain: IOMM-Lee. Neurosurgery 1990;27(3):389-96.

25. Mei Y, Bi WL, Greenwald NF, Agar NY, Beroukhim R, Dunn GP, et al. Genomic profile of human meningioma cell lines. PloS One 2017;12(5):e0178322.

26. Chandran K, Sullivan NJ, Felbor U, Whelan SP, Cunningham JM. Endosomal proteolysis of the Ebola virus glycoprotein is necessary for infection. Science 2005;308(5728):1643-5.

27. Wollmann G, Drokhlyansky E, Davis JN, Cepko C, van den Pol AN. Lassa-vesicular stomatitis chimeric virus safely destroys brain tumors. J Virol 2015;89(13):6711-24.

28. Dulbecco R, Vogt M. Some problems of animal virology as studied by the plaque technique. Cold Spring Harb Symp Quant Biol 1953;18:273-9.

29. Lawson ND, Stillman EA, Whitt MA, Rose JK. Recombinant vesicular stomatitis viruses from DNA. Proc Natl Acad Sci USA 1995;92(10):4477-81.

30. Gallione CJ, Rose JK. A single amino acid substitution in a hydrophobic domain causes temperature-sensitive cell-surface transport of a mutant viral glycoprotein. J Virol 1985; 54(2):374-82.

31. Duffy S. Why are RNA virus mutation rates so damn high? PloS Biol 2018;16(8):e3000003.

32. Steinhauer DA, Domingo E, Holland JJ. Lack of evidence for proofreading mechanismsassociated with an RNA virus polymerase. Gene 1992;122(2):281-8.

33. Elena SF, Miralles R, Cuevas JM, Turner PE, Moya A. The two faces of mutation: Extinction and adaptation in RNA viruses. IUBMB Life 2000;49(1):5-9.

34. Drake JW, Holland JJ. Mutation rates among RNA viruses. Proc Natl Acad Sci USA 1999; 96(24):13910-3.

35. Davis JN, van den Pol AN. Viral mutagenesis as a means for generating novel proteins. J Virol 2010;84(3):1625-30.

36. Kretzschmar E, Peluso R, Schnell MJ, Whitt MA, Rose JK. Normal replication of vesicular stomatitis virus without C proteins. Virology 1996;216(2):309-16.

37. Akpinar F, Timm A, Yin J. High-throughput single-cell kinetics of virus infections in the presence of defective interfering particles. J Virol 2015;90(3):1599-612.

38. Lyles DS, Rupprecht CE. *Rhabdoviridae.* In: Knipe DM & Howley PM, editors. Fields Virology 5th Edition. Philadelphia: Lippincott Williams & Wilkins; 2007. p. 1363-408.

39. Lam V, Duca KA, Yin J. Arrested spread of vesicular stomatitis virus infections in vitro depends on interferon-mediated antiviral activity. Biotechnol Bioeng 2005;90(7):793-804.

40. Osada N, Kohara A, Yamaji T, Hirayama N, Kasai F, et al. The genome landscape of the African green monkey kidney-derived Vero cell line. DNA Res 2014;21(6):673-83.

41. Kawamura Y, Hua L, Gurtner A, Wong E, Kiyokawa J, *et al.* Histone deacetylase inhibitors enhance oncolytic herpes simplex virus therapy for malignant meningioma. Biomed Pharmacother 2022;155:113843.

42. Jeetendra E, Robison CS, Albritton LM, Whitt MA. The membrane-proximal domain of vesicular stomatitis virus G protein functions as a membrane fusion potentiator and can induce hemifusion. J Virol 2002;76(23):12300-11.

43. White JM, Whittaker GR. Fusion of enveloped viruses in endosomes. Traffic 2016;17(6):593-614.